

Jet areas as a tool for background subtraction

Grégory Soyez^{1,a}

¹ Brookhaven National Laboratory, Building 510, NY 11973 Upton, USA

Abstract. In all modern hadronic colliders, jets receive a large contribution from a soft background: pileup in the case of proton-proton collisions at the LHC, or the underlying event for heavy-ion collisions at RHIC or the LHC. In these proceedings, we present a generic and simple method, based on jet areas, to subtract the contribution of the soft background from the jets. This allows for more precise kinematic reconstruction of jets in dense environments.

Keywords: Jets, QCD
PACS: 12.38.Aw, 12.38.Bx

1. Introduction

In all recent colliders, jets have been useful objects in numerous analysis involving large- p_t hadrons in the final state. However, with the high-luminosity expected at the LHC as well as with the large multiplicities obtained in heavy-ion collisions at RHIC, jets get significant contributions from the soft background leading to biased measures of their momentum.

For all the analysis involving jets, it is important to determine as well as possible their kinematic properties. therefore, one has to develop techniques allowing to deal with the soft-background contribution to the jet.

In these proceedings, we discuss soft background subtraction using jet areas. The underlying idea to this method is that, by suitably defining what the area of a jet is, the contamination due to soft background will be proportional to it.

We shall start by giving two possible definitions of the concept of the area of a jet and show that those definitions allow for analytic computations in perturbative QCD. We shall then explain how one can use the jet area to subtract background contamination.

Details concerning the definition of jet areas and their properties can be found in [1], and the application to background subtraction in [2].

2. Jet areas

2.1. Definition

Keeping in mind that we ultimately want to use jet areas in order to correct from soft-background contamination, we aim at a definition that mimics the reaction of the jet to soft particles. To do that in practice, we will introduce additional, infinitely soft, particles that we shall refer to as *ghosts*. For infrared-safe algorithm, the addition of ghosts will not alter the clustering. We can then define the area of a jet as the region in rapidity-azimuth where it catches ghosts.

We can consider two different ways of doing this:

- **Passive area:** the passive area is defined as the region in which a jet would catch a single ghost added to the event.
- **Active area:** in this case, we add to the event a set of ghosts $\{g_i\}$, with density per unit area ν_g . If n_J ghosts are clustered with a jet J , its area w.r.t. to that set of ghosts will be n_J/ν_g . We then define the active jet area of J as the limit of $\langle n_J/\nu_g \rangle$, averaged over all ghosts distributions, when ν_g goes to infinity, *i.e.* in the limit of infinitely dense ghost coverage. Note that in this case, one can also end up with jets only made of ghosts.

Both the passive and the active area can easily be defined as 4-vectors. Those are formally defined by summing (or more precisely integrating) the momenta of all the ghosts contributing to the area of a jet, normalised in such a way that its transverse momentum corresponds to the scalar area.

Physically speaking, the passive area which clusters a single ghost at a time has similar behaviours as a point-like background, while the active areas correspond to diffuse, uniform, backgrounds.

A final comment concerns the jet algorithm choice. Since the definitions of jet areas given in this Section involve adding soft particles, it is of prime importance that these ghosts do not modify the clustering of the hard particles in the original event, a property known as infrared-safety. In what follows, we shall consider 4 infrared-and-collinear-safe algorithms: the k_t [4], Aachen/Cambridge [5] and anti- k_t [6] algorithms as well as SISCone [7].

2.2. Perturbative properties

In this Section, we briefly highlight some nice perturbative properties that can be explicitly computed for jet areas. The quantity we shall be interested in is the average active and passive area of a jet at the first non-trivial order in α_s *i.e.* including the radiation of a gluon. We will work in the soft-collinear limit that is relevant for small values of R and properly take into account the running of the QCD coupling constant.

The first step is to start with the area of a hard jet made of a single particle of transverse momentum p_{t1} . The case of passive areas is particularly simple: for every

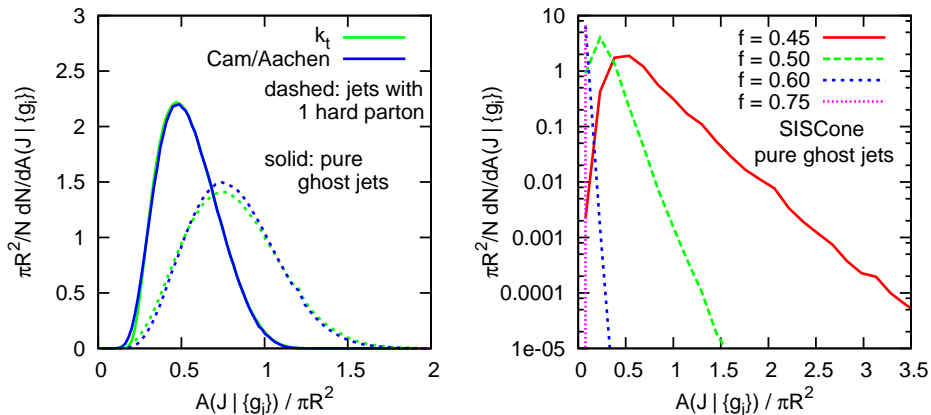


Fig. 1. Distribution of the active areas for a hard jet made of a single hard particle and the pure-ghost jets. Left: k_t and Aachen/Cambridge, right: SIScone.

algorithm, an infinitely soft particle will be clustered with the hard one if-and-only-if it is at most at a distance R from it, hence an area of πR^2 .

The case of active areas is a bit more subtle. For the anti- k_t algorithm, ghost recombinations with the hard particle will happen at the very beginning of the cluster sequence, resulting in a area of πR^2 . For SIScone, one first has to notice that the stable cones in the event made with a single hard particle and a dense ghost coverage are (i) the cone centred on the hard particles and (ii) any cone made only of ghosts. Through the split–merge phase, the overlapping between the hard stable cone and all the pure-ghost ones, with centres approaching the hard one up to a distance R , will lead to a splitting (for $f \gtrsim 0.4$), leading to a cone of radius $R/2$ as the final jet, hence an area of $\pi R^2/4$. Finally, in the case of the k_t and Cambridge algorithms, ghosts will also cluster among themselves leading to different areas for different sets of ghosts. On average, one finds an area around $0.81\pi R^2$ for both k_t and Aachen/Cambridge (with respective dispersions of $0.28\pi R^2$ and $0.26\pi R^2$).

The distribution areas for the hard jet and the pure-ghost jets are presented in Figure 1. Note that for SIScone, for small values of the overlap threshold there is a substantial probability that pure-ghost jets become very large (known as *monster jets*). To avoid this, larger values of f can be chosen. This kind of arguments suggests $f = 0.75$ as a sensitive default.

Next, we proceed with the computation of jet areas for situations with a hard particle of transverse momentum p_{t1} and a softer one with transverse momentum $p_{t2} \ll p_{t1}$ located at a distance Δ from the first one. The calculation of the area as a function of Δ goes typically as for the 1-particle case, though with slightly more involved geometry, so we will not detail the results here (see [1] for details). In the case of the passive area, one can perform all the computations analytically,

	$a_{\text{JA,1hard}}$		d_{JA}	
	passive	active	passive	active
k_t	1	0.81	0.56	0.52
Cam/Aachen	1	0.81	0.08	0.08
anti- k_t	1	1	0	0
SISCone	1	1/4	-0.06	0.12

Table 1. Summary table giving the one-particle average area and the scaling violation coefficients for the passive and active areas and for various jet algorithms. All quantities correspond to an area divided by πR^2 .

while for passive areas, anti- k_t and SISCone are treatable analytically but we once again have to rely on numerical simulations to account for the ghost-distribution dependence in the two remaining cases.

The important point is that, once we have the results for 1 and 2 particle jets, we can compute the average area of a jet perturbatively at order α_s . At leading order, a jet is made of a single parton, while at next-to-leading order in α_s , an extra gluon can be radiated. For a jet definition JD one thus has

$$\langle A_{\text{JD}} \rangle \simeq \langle A_{\text{JD}} \rangle_{\text{1hard}} + \int d\Delta \int_{Q_0/\Delta}^{p_{t1}} dp_{t2} \frac{dP}{d\Delta dp_{t2}} \left(\langle A_{\text{JD}}(\Delta) \rangle_{\text{2part.}} - \langle A_{\text{JD}}(0) \rangle_{\text{2part.}} \right),$$

where the last term receives a 2-particle contribution from real-gluon emissions and a 1-particle virtual correction. Since the p_{t2} integration has a soft divergence — coming from the gluon-radiation probability — one has to introduce a cut-off. The value Q_0/Δ above comes by requiring that the transverse momentum of the emitted gluon relative to its parent, *i.e.* $p_{t2}\Delta$ in the small-angle approximation, is larger than the soft cut-off Q_0 . We will come back to the importance of this cut-off later on.

In the soft and collinear approximation, the probability for gluon emissions is

$$\frac{dP}{d\Delta dp_{t2}} = C_R \frac{2\alpha_s(p_{t2}\Delta)}{\pi} \frac{1}{\Delta} \frac{1}{p_{t2}}$$

with the colour factor C_R is C_F or C_A for quark and gluon jets respectively. Again, the argument of the coupling is the transverse momentum of the second particle relative to the first one.

The final result, normalised by πR^2 , can be cast under the form

$$\frac{\langle A_{\text{JD}} \rangle}{\pi R^2} \simeq a_{\text{JA,1hard}} + d_{\text{JA}} \frac{C_R}{b_0\pi} \log \left(\frac{\alpha_s(Q_0)}{\alpha_s(Rp_{t1})} \right), \quad (1)$$

where $b_0 = (11C_A - 2n_f)/(12\pi)$ is the one-loop QCD beta-function, and we have neglected terms that were not logarithmically enhanced. To grasp the physical content of this equation, a few comments are in order:

- The coefficients $a_{\text{JA,1hard}}$ and d_{JA} , related to the one-particle area and the one-gluon emission corrections respectively, depend on the chosen algorithm JA and area type. They can both be analytically computed from the one and two-particle situations mentioned above. A summary of the relevant values is presented in Table 1.
- Not only the area of a jet is not always πR^2 as one might naively expect — we already noticed that earlier — but eq. (1) shows that the jet substructure generates some scaling violations.
- Because of the prefactor C_R , the scaling violations will be larger for gluon jets than for quark jets.
- The cut-off Q_0 is a non-perturbative scale. It is the trace that, since the addition of a soft particle can modify them, jet areas are not infrared-safe quantities. Physically, they should be regularised by a scale related to the underlying event density in pp or heavy-ion collisions, or by the pileup density in the presence of pileup. It is interesting to notice that, as long as we keep the limit $p_{t1} \gg Q_0$, the scaling violations reduce when increasing the background density.
- In the specific case of the anti- k_t algorithm, the coefficient $d_{\text{anti-}k_t}$ vanishes. Actually, in the limit of soft emissions, this is true at any order and the area remains πR^2 , a fact reminiscent of the rigidity of the algorithm. The correction to that result will only come with power-suppressed factors, without logarithmic enhancement.

2.3. Implementation

In practice, jet areas have been implemented in **FastJet**[3]. Ghosts are placed on a square grid with each node slightly shifted. The binning of that grid, corresponding to the quantum of area carried by each ghost, can be specified to achieve the desired accuracy. The computation can also be averaged over different ghosts distributions, *i.e.* different shifts of the grid.

3. Background subtraction

We finally come to the question of how jet areas can be used to subtract jet contamination from soft background. For simplicity, we shall concentrate on the case of a background uniform over a rapidity range $|y| \leq y_{\text{max}}$. If the background has a density per unit area ρ , the subtraction formula for a given jet is the following:

$$p_{\text{subtracted}}^\mu = p_{\text{jet}}^\mu - \rho A_{\text{jet}}^\mu, \quad (2)$$

where A^μ is the jet 4-vector area. We discuss below the two building blocks of this formula, namely the jet area and the background density.

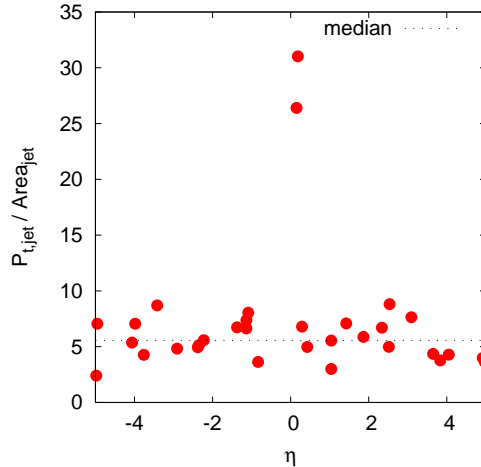


Fig. 2. Example of the distribution of p_t/area of the jets for one specific example. The lower points are pure-background jets while the 2 upper ones are the hard jets.

3.1. The jet area

This point has already been addressed in Section 2. Given the fact that the background is uniform, active areas are a natural choice. However, for large multiplicities, the passive area tends to the active one, so the passive area can also be used. This might be relevant *e.g.* for SISCone as the computation of passive areas is much less time-consuming than the one of active areas.

3.2. The medium density per unit area

We are left with the estimation of the background density per unit area. The estimation we propose here is based on the observation that the ratio of the p_t of a jet divided by its area can behave in two distinctive ways: it will be around ρ for the many jets made purely of background, and much larger for the few hard jets. As a consequence, the median of the set of p_t/area for all the jets in the event gives an estimate of the background density ρ . This is illustrated in Figure 2.

A tricky point here is that we optimally want to avoid having too many jets with small area as it would lead to large uncertainties in p_t/area . In that respect, the k_t and Cambridge/Aachen algorithms are the best suited choices. This means that, whatever algorithm you plan on using and apply the subtraction method, it is advised to pre-estimate ρ using k_t or Cambridge/Aachen, and then use that value of ρ to perform the subtraction with the chosen algorithm.

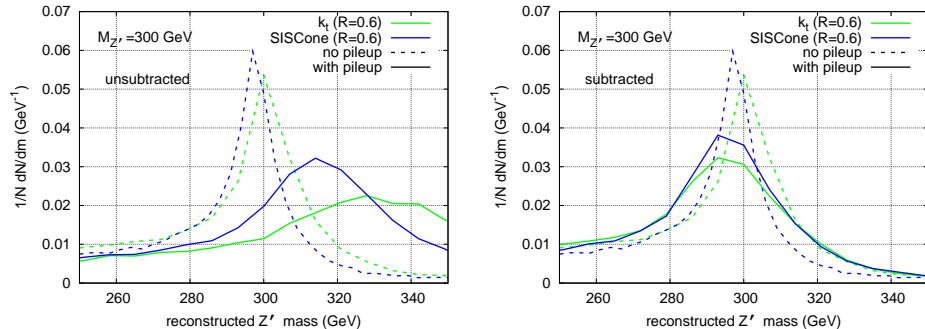


Fig. 3. Left: reconstruction of the Z' mass peak without pileup (dashed lines) and with pileup without applying subtraction (solid lines). Right: same except that our subtraction method has been applied in the case where pileup was added. Both cases are presented for the k_t and SISConé algorithms with a radius of 0.6.

3.3. Properties and applications

An essential point here is that this subtraction method can be applied individually for each event. The main advantage is that it significantly reduces the event-by-event fluctuations of the density of the background, reducing its smearing effects.

In addition, the method is simple and general enough to have a broad range of applications, ranging from pileup subtraction in pp collisions to underlying-event subtraction in pp or AA collisions. See *e.g.* [8] for an explicit experimental application by STAR for AA collisions at RHIC.

Finally, let us illustrate the effects of subtraction on a simple example. We have generated with Pythia 6.4 (tune DWT), a set of fictitious Z' events, where the Z' has a mass fixed to 300 GeV (with a narrow width of less than 1 GeV) and decays into a $q\bar{q}$ pair^b. The events are clustered and the two hardest of the resulting jets, the best candidates to match the original quark and anti-quark, are used to reconstruct the Z' . We can study how the mass peak of the Z' is reproduced in 3 different cases:

1. without pileup addition,
2. with pileup, simulated by adding minimum bias events with a Poissonian distribution corresponding to a luminosity of 0.25 mb^{-1} per bunch crossing (LHC at designed luminosity),
3. with pileup and applying the subtraction method presented here.

The results of the reconstruction of the Z' mass peak are presented in figure 3 without pileup subtraction on the left and with pileup subtraction on the right. In both cases, we show the results when the k_t and SISConé algorithms with a radius of 0.6 are used for the clustering. The subtraction on the right plot has been done

using (2) where ρ is estimated using the k_t algorithm with a radius of 0.5, keeping all the jets with $|y| < 5$. While without subtraction the position of the peak is severely shifted towards larger masses and its width is much larger, after applying our subtraction technique, the peak comes back to a good position and its width, though a bit larger than without pileup, is much reduced compared to what we had before subtraction.

Acknowledgements

I am very grateful to Matteo Cacciari and Gavin Salam for collaboration on the topics presented in these proceedings.

Note(s)

- a.* Supported by Contract No. DE-AC02-98CH10886 with the U.S. Department of Energy.
E-mail: gsoyez@quark.phy.bnl.gov
- b.* Such a small mass for a potential Z' has already been excluded. However, we use it here simply as a source of dijets at a fixed scale.

References

1. M. Cacciari, G. P. Salam and G. Soyez, *JHEP* **0804** (2008) 005 [[arXiv:0802.1188](https://arxiv.org/abs/0802.1188)].
2. M. Cacciari and G. P. Salam, *Phys. Lett.* **B659** (2008) 119 [[arXiv:0707.1378](https://arxiv.org/abs/0707.1378)].
3. M. Cacciari and G. P. Salam, *Phys. Lett. B* **641** (2006) 57 [[arXiv:hep-ph/0512210](https://arxiv.org/abs/hep-ph/0512210)]; M. Cacciari, G. P. Salam and G. Soyez, <http://www.fastjet.fr>
4. S. Catani, Y. L. Dokshitzer, M. H. Seymour, and B. R. Webber, *Nucl. Phys.* **B406** (1993) 187; S. Catani, Y. L. Dokshitzer, M. Olsson, G. Turnock, and B. R. Webber, *Phys. Lett.* **B269** (1991) 432; S. D. Ellis and D. E. Soper, *Phys. Rev.* **D48** (1993) 3160–3166, [[hep-ph/9305266](https://arxiv.org/abs/hep-ph/9305266)].
5. Y. L. Dokshitzer, G. D. Leder, S. Moretti, and B. R. Webber, *JHEP* **08** (1997) 001, [[hep-ph/9707323](https://arxiv.org/abs/hep-ph/9707323)]; M. Wobisch and T. Wengler, [hep-ph/9907280](https://arxiv.org/abs/hep-ph/9907280).
6. M. Cacciari, G. P. Salam and G. Soyez, *JHEP* **0804** (2008) 063 [[arXiv:0802.1189](https://arxiv.org/abs/0802.1189)].
7. G. P. Salam and G. Soyez, *JHEP* **05** (2007) 086, [[arXiv:0704.0292](https://arxiv.org/abs/0704.0292)]; see also, <http://projects.hepforge.org/siscone>.
8. S. Salur, [arXiv:0905.1917](https://arxiv.org/abs/0905.1917), contribution to these proceedings.